Moringua edwardsi (Moringuidae: Anguilliformes): Cranial Specialization for Head-First Burrowing?

N. De Schepper,* D. Adriaens, and B. De Kegel

Ghent University, Evolutionary Morphology of Vertebrates, 9000 Ghent, Belgium

ABSTRACT   The order Anguilliformes forms a natural group of eel-like species. *Moringua edwardsi* (Moringuidae) is of special interest because of its peculiar fossorial lifestyle: this species burrows head-first. Externally pronounced morphological specializations for a fossorial lifestyle include: reduced eyes, lack of color, low or absent paired vertical fins, elongated, cylindrical body, reduced head pores of the lateral line system, etc. Many fossorial amphibians, reptiles, and even mammals have evolved similar external specializations related to burrowing. The present study focuses on osteological and myological features of *M. edwardsi* in order to evaluate the structural modifications that may have evolved as adaptations to burrowing. Convergent evolutionary structures and possible relations with head-first burrowing, miniaturization, feeding habits, etc., were investigated. Body elongation, reduction of the eyes, modified cranial lateral line system, and modified skull shape (pointed though firm) can be considered specializations for head-first burrowing. Hyperossification can probably be regarded more as a specialization to both head-first burrowing and feeding, even though an impact of miniaturization cannot be excluded. Hypertrophied adductor mandibulae muscles and the enlarged coronoid process can be associated with both feeding requirements (it enhances bite forces necessary for their predatory behavior) and with a burrowing lifestyle, as well as miniaturization. J. Morphol. 266:356–368, 2005.   © 2005 Wiley-Liss, Inc.

KEY WORDS: Anguilliformes; convergent evolution; adaptation; burrowing; cranial morphology

Moringua edwardsi belongs to the family Moringuidae (Anguilliformes; Regan, 1912; Nelson, 1994). They are commonly known as spaghetti eels. Despite the common features shared with other Anguilliformes, this species caused considerable confusion in the past because of its striking ontogenetic polymorphism. Many different ontogenetic stages were even described as distinct genera (Smith and Castle, 1972). Moringuidae appear to be phylogenetically related to Anguillidae and Heterenchelidae (Smith, 1989a). According to Smith (1989a), Moringuidae share pronounced morphological specialization for a fossorial lifestyle with Heterenchelidae and Ophichthidae: reduced eyes, lack of color, low vertical fins, elongated, cylindrical body, and reduced head pores. In contrast to tail-first burrowing Ophichthidae species, both Heterenchelidae and

Moringuidae burrow head-first (Castle, 1968; Smith and Castle, 1972; Smith, 1989a). It is striking that only immature specimens of *M. edwardsi* spend all their time burrowed in the sand (Gordon, 1954; Gosline, 1956). Adults seem to limit their burrowing behavior, as they leave their burrows during the night (Smith, 1989a). Smith (1989a) mentions rapid movements of the body, just beneath the surface, for subterranean hunting and feeding. The modification of the snout into a solid conical structure, combined with a protruding lower jaw, facilitate burrowing, where power is provided by the cylindrical body (Castle, 1968; Smith, 1989a). As immature specimens spend most of their time buried in the sand, they form the most obvious study object to examine the degree of structural specializations for burrowing. In this study, a detailed description of the cranial osteological and cranial myological features of such immature moringuids (*M. edwardsi*) was performed. The detailed morphology of the head was examined with the goal to apportion the anatomical specializations among head-first burrowing, miniaturization, and predatory feeding.

MATERIALS AND METHODS

For this study three alcohol-preserved immature specimens of *Moringua edwardsi* (MCZ 44686) were used, obtained from the Museum of Comparative Zoology (Harvard University, Cambridge, MA): ME1: total length (TL) = 219.17 mm; ME2: TL = 200.07 mm; and ME3: TL = 171.72 mm. One specimen (ME2) was cleared and stained with Alizarin red S and Alcian blue according to the protocol of Hanken and Wassersug (1981). This specimen was studied by means of a stereoscopic microscope (Olympus SZX-9), equipped with a camera lucida and a Colorview 8 digital camera. To determine the detailed morphology of the head skeleton of this small fish, serial histological cross sections were studied. Specimens were fixed with formaldehyde solution (8%), decalcified with Decalc 25% (HistoLab, Gothenburg, Sweden), dehydrated through an alcohol series, and embedded in Technovit
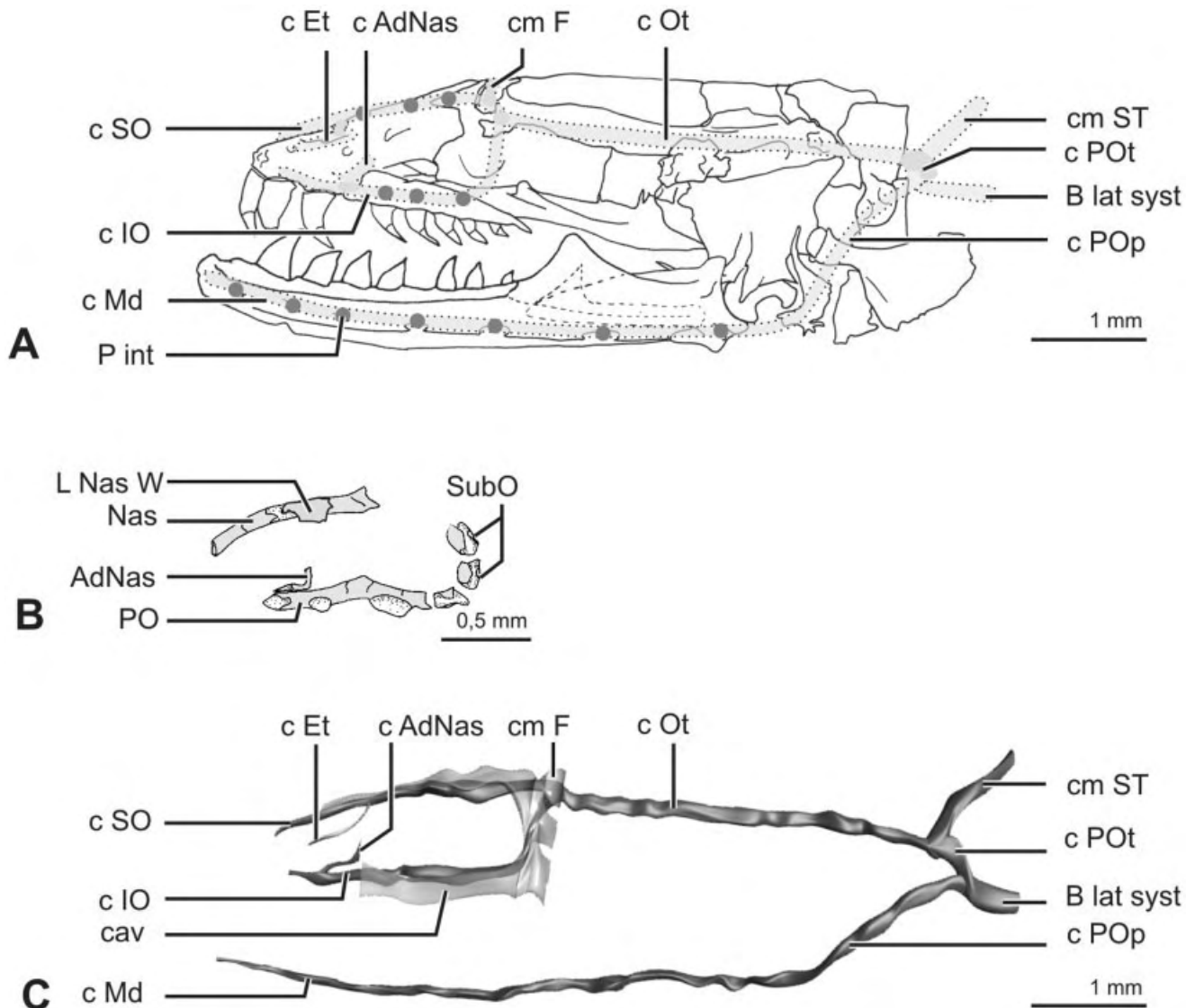
Fig. 1. The cranial lateral line system of *Moringua edwardsi*. **A:** Lateral view of the composing canals. Dark dots illustrate internal sensory pores. The orbital pores are in contact with the dermal cavities. **B:** Lateral view of circumorbital bones of the cranial lateral line system. **C:** 3D reconstruction of the cranial lateral line system, with position of the dermal cavities.

7100 (Kulzer-Heraus). Series of semithin sections (2 μm) were cut using a Leica Polycut SM 2500, stained with Toluidine blue, and mounted with DPX. Images of the sections were obtained using a digital camera (Colorview 8, Soft Imaging System, Munster, Germany) mounted on a light microscope (Polyvar, Reichert, Jung, Austria) and processed with Analysis Docu (Soft Imaging System, v. 3.0). Based on the serial histological sections, a 3D reconstruction was generated using Corel-Draw 8 (Corel, Canada) for tracing contours of the structures and Rhinoceros 3.0 (McNeel, Seattle, WA) for making reconstructions based on NURBS (Fig. 1C). Abbreviations used are alphabetically ordered in Table 1. Nomenclature of cranial skeletal elements follows that of Gregory (1933). Terminology of skeletal elements of the caudal fin follows that of Gosline (1965), Monod (1968), and Lundberg and Baskin (1969). The terminology of the musculature follows Winterbottom (1974). Terminology used to define sutures and articulations follows Hildebrand (1995). Obtained osteological data are compared with previous articles by Trewavas (1932) and Smith (1989a).

RESULTS
Cranial Lateral Line System

The cranial lateral line system comprises the supra- and infraorbital canals, the otic canal, the postotic canal, the mandibular canal and the preopercular canal, the ethmoid canal, the adnasal canal, the frontal commissure, and the supratemporal commissure (Fig. 1A). The supra- and infraorbital canals are mainly supported by the following circumorbital bones: a large nasal, small adnasal, long preorbital, and three suborbitals (Fig. 1B). The nasal bone comprises three ossicles. The first and anterior part of the nasal is tube-like and lies in front of the olfactory organ. The second part of the nasal bone, covering the dorsal roof of the olfactory organ,

TABLE 1. Alphabetical list of abbreviations used in drawings

A1, 2, 3 Aω	parts of the adductor mandibulae complex	L BH-CH	basihyal-ceratohyal ligament
A2d, m, v	dorsal, medial and ventral part of A2	L Hm-CH	hyomandibula-ceratohyal ligament
AAP	adductor arcus palatini	L IOp-CH	interopercular-ceratohyal ligament
ac Md	mandibular articular condyle	L Nas W	lateral nasal wings
ac Op	opercular articular condyle	L Op-IOp	operculo-interopercular ligament
ac susp A	anterior suspensorial condyle	L POp-Op	preoperculo-opercular ligament
ac susp P	posterior suspensorial condyle	L PP	palatopterygoidal ligament
AdNas	adnasal	L prim	primordial ligament
af Mx-Etv A	anterior maxillo-ethmovomerine articulation facet	L UH-CH	urohyal-ceratohyal ligament
af Mx-Etv P	posterior maxillo-ethmovomerine articulation facet	LAP	levator arcus palatini
af Op	opercular articular facet	LO	levator operculi
af susp A	anterior suspensorial articulation facet	Mx	maxillary
af susp P	posterior suspensorial articulation facet	Nas	nasal
AH	adductor hyomandibulae	Op	operculum
Ang	angular complex	Orb	orbits
AO	adductor operculi	P int	internal pore
apo	aponeurosis	Par	parietal
B lat syst	body lateral line system	PH	protractor hyoidei
BH	basihyal	PHα	ventral part of the protractor hyoidei
BOc	basioccipital	PHβ	dorsal part of the protractor hyoidei
c AdNas	adnasal canal	PMx-Etv	premaxillo-ethmovomerine complex
c Et	ethmoid canal	PO	preorbital
c IO	infraorbital canal	POp	preoperculum
c Md	mandibular canal	PP	palatopterygoid
c Ot	otic canal	Pr cor	coronoid process
c POp	preopercular canal	pr D Op	dorsal opercular process
c POt	postotic canal	Pr PSph	parasphenoid process
c SO	supraorbital canal	Pro	prootic
cav	dermal cavity	PSph	parasphenoid
CH A	anterior ceratohyal	Pt	pterotic
CH P	posterior ceratohyal	PtSph	pterosphenoid
cm F	frontal commissure	Q	quadrate
cm ST	supratemporal commissure	R Br	branchiostegal rays
CM	coronomeckelian	SH	sternohyoideus
ct	connective tissue	SOc ri	supraoccipital ridge
D	dentary complex	SOc	supraoccipital
DO	dilatator operculi	SOp	suboperculum
Epax	epaxial muscle	Sph	sphenotic
Epi	epiotic	SubO	suborbital
ExOc	exoccipitals	T A2m, v	tendon of A2m and A2v
F	frontal	T DO	tendon of dilatator operculi
FA	frontal arch	T LAP	tendon of levator arcus palatini
Fas A2	fascia connecting counterparts of A2m	T LO	tendon of levator operculi
HH	hyohyoideus	T PH A	anterior tendon of protractor hyoidei
Hm	hyomandibula	T PHα P	posterior tendon of ventral part of PH
Hyp	hypaxial	T PHβ P	posterior tendon of dorsal part of PH
IOp	interoperculum	T SH	tendon of sternohyoideus
L Ang-IOp	angulo-interopercular ligament	UH	urohyal
L Ang-POp	angulo-preopercular ligament		

has a horizontal position. The medial side of this part contains the supraorbital canal, while thin wings expand laterally. Behind the nasal sac, the third part of the nasal is again tube-like, lacking the horizontal plates. The supraorbital canal has an ethmoid canal, running ventrally and enclosed by the premaxillo-ethmovomerine complex. Behind the nasals, the supraorbital canal is enclosed by the frontal. More caudally it is partially enclosed by incomplete extensions or arches of the frontal. The frontal commissure connects the left and right supraorbital canal (Fig. 2A). The rostral part of the infraorbital canal is enclosed in the preorbital. The dorsal adnasal canal is enclosed by the adnasal. Behind the eyes, the infraorbital canal is surrounded by three suborbitals and meets the supraorbital canal (Fig.

2Ba). Both fuse in the anterior process of the pterotic, continuing as the otic canal. This otic canal is enclosed by the pterotic and runs up to the caudal part of the skull. The mandibular canal is enclosed by the dentary complex (Fig. 2C). Posterior to the mandibular articulation the preopercular canal is enclosed by the preoperculum. The otic canals are connected through a supratemporal commissure. The bases of this commissure are situated in front of the fusion of the preopercular canal and the otic canal (no longer surrounded by the pterotic) (Fig. 2D) into the postotic canal, which is consequently very short.

No external head pores are present, implying that the cranial lateral line system is not connected to the environment, at least in the head region. However, the circumorbital bones (nasal, adnasal, preor-
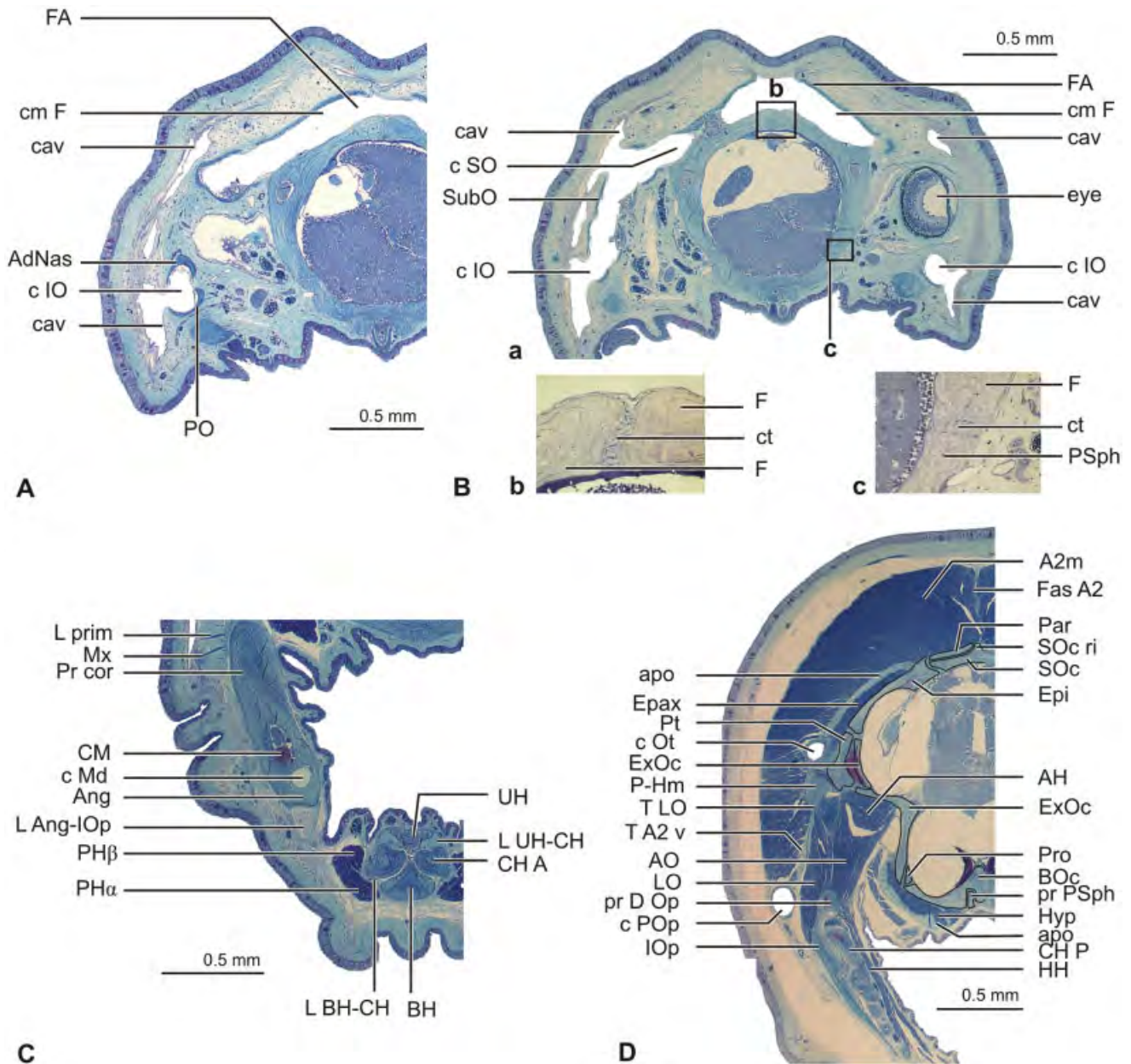
Fig. 2. **A:** Cross section of the head of *Moringua edwardsi* at the level of the frontal commissure. **Ba:** Cross section at the level of the fusion between the supra- (c SO) and infraorbital canal (c IO). Inserts show scarf joints and connective tissue (ct) between frontals (**Bb**) and between frontals and parasphenoid (PSph) (**Bc**). **C:** Cross section at the level of the hyoid apparatus. **D:** Cross section at the level of the occipital region. Lines surrounding the bones are manually drawn to improve the visualization of the borderlines.

bital, and suborbitals), as well as the dentary complex, are pierced by many internal pores (Fig. 1A). These pores lead to interconnected, dermal cavities, situated lateral to and along the total length of the supra- and infraorbital canals (Figs. 1C, 2A,Ba). It is remarkable that these cavities are not connected with any external pores or with the environment. Neuromasts are observed in all canals and are well developed.

The eyes of the immature specimens are very small, dark spots and are covered with semi-opaque skin (Fig. 2Ba). The orbits, which enclose the eyes, are small as well (Fig. 3A).

Osteology

The neurocranium is heavily ossified, forming one solid unit, with the exception of a movable maxillary (Fig. 3A,B). The shape of the neurocranium is elongate, tapering from its widest part, the otic region, toward the tip of the snout. The orbits are small. Large recurved teeth are present and supported by
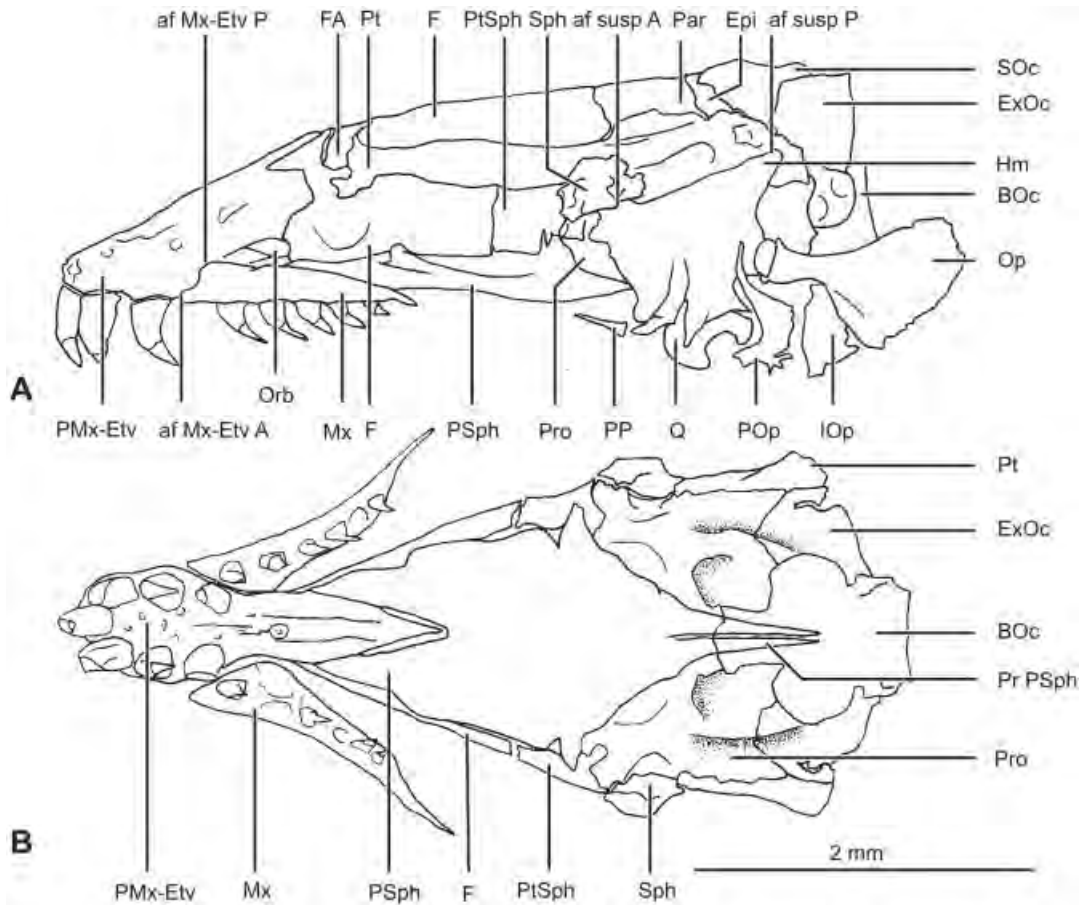
Fig. 3. Illustration of the position of the cranial bones of *Moringua edwardsi* in (**A**) lateral view and (**B**) ventral view.

the premaxillo-ethmovomerine complex, maxillary, and lower jaw. Tooth size decreases caudally. Neighboring bones are interconnected by connective tissue and form scarf joints (Fig. 2Ba,b). The bones forming the skull roof (frontals, parietals, supraoccipital, epiotics, and exoccipitals) show a high amount of overlap, formed by the extension of the scarf joint (Fig. 4B) (terminology [scarf joint] follows Hildebrand, 1995). Both frontals show less extended scarf joints between each other, although the scarf joints between the frontals and parietals are extremely extended.

The ethmoid region comprises the premaxilloethmovomerine complex and the nasals. The latter are described with respect to the lateral line system (Fig. 1). A robust and compact premaxilloethmovomerine complex is present, forming the rostral tip of the neurocranium. Two small, cartilaginous nasal bars are situated ventral to the nasal organ and lateral to the premaxillo-ethmovomerine complex. These cartilaginous nasal bars contact the premaxillo-ethmovomerine complex posteriorly. These bars aid in support of the nasal organ. Lateral to the complex, robust but elongate maxillaries are present. The anterior part of the maxillary bears

small ventral and dorsal processes, which rest in the anterior and posterior maxillo-ethmovomerine articular facets on the premaxillo-ethmovomerine complex, respectively. The posterior end of the maxillary is surrounded by the primordial ligament, which attaches to the dorsolateral face of the lower jaw (Fig. 2C).
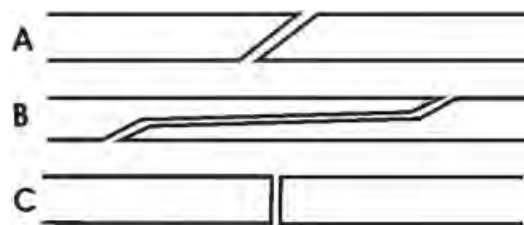

Fig. 4. Schematic illustration of joint types between skull bones in *Moringua edwardsi*. **A:** Scarf joint—The cranial bones are connected by connective tissue and form scarf joints, with tapering edges. **B:** Extended scarf joint—The cranial bones of skull roof (frontals, parietals, supraoccipital, epiotics, and exoccipitals) show a high amount of overlap, formed by the extension of the scarf joints. The frontals are interconnected by scarf joints and connected to the parietals by extended scarf joints. **C:** Butt joint—These have straight sutures and nearly square edges.

The orbital region comprises the pterosphenoids, frontals, adnasals, preorbitals, and suborbitals. Orbitosphenoid and basisphenoid are absent. The paired frontals meet in the midline and are strongly interconnected by a scarf joint (Fig. 2Bb). Connective tissue is present between both bones. Anteriorly, the frontals border the posterior edge of the premaxillo-ethmovomerine complex. The pterotics cover the frontals caudolaterally. The caudoventral part contacts the parasphenoid ventrally and the pterosphenoid caudally, all as a result of scarf joints (Fig. 2Bc). The caudodorsal parts of the frontals overlie the parietals caudally, as a result of extreme extension of the scarf joint. Part of the supraorbital canal runs in incompletely expanded canals formed by frontal extensions, referred to as frontal arches (Fig. 2Ba). More caudally, this canal is completely enclosed in the frontal. The pterosphenoid contacts the pterotic dorsally and the parasphenoid ventrally. Again, scarf joints connect these bones. Preorbital, suborbitals, and adnasal are described with respect to the lateral line system (Fig. 1).

The otic region comprises the sphenotics, pterotics, prootics, epiotics, and parietals, in which all neighboring bones are connected by scarf joints. The ventral surface of the sphenotic contacts the dorsolateral side of the prootic, forming the anterior articular groove, or dilatator fossa for the connection between the hyomandibula. The lateral sphenotic process is supported by a bony strut, which is partially formed by the anterodorsal surface of the prootic and partially by the sphenotic. This process contributes to the anterior suspensorial articular facet. The pterotic forms the lateral wall of the skull and contains the otic canal. The dorsal edge connects to the frontal, parietal, epiotic, and exoccipital. Ventrally, it contacts the frontal, the pterosphenoid, the sphenotic, the prootic, and exoccipital. Caudally, the posterior suspensorial articular facet contributes to the articulation between the suspensorial hyomandibula and the neurocranium. The prootic forms the anterior part of the otic bullae. The dorsal edge of the prootic abuts the pterosphenoid, the sphenotic, and pterotic. Ventrally, it connects the parasphenoid and the basioccipital. The pterotic and the prootic form an articulating groove for the dorsal edge of the hyomandibulo-quadrate. The epiotics are connected to the supraoccipital and exoccipital, and their anterior parts contact the pterotic and parietals. The first third of the parietals is overlaid by the frontals, thus forming an extended scarf joint. A scarf joint connects both parietals. The parietals overlie the supraoccipital caudally (Fig. 2D) and the epiotics.

The occipital region comprises the exoccipitals, basioccipital, supraoccipital, and parasphenoid, which are connected by connective tissue, forming scarf joints. The anterior part of the exoccipitals contacts the pterotic dorsally and the prootics ventrally. The medial part joins the supraoccipital dorsally and the basioccipital ventrally, whereas both exoccipitals interconnect posteromedially. The foramen magnum is surrounded by the exoccipitals laterally and dorsally. The occipital region is dominated by the basioccipital (Fig. 3B). The basioccipital and prootic are expanded, forming the posterior part of a large otic bulla. The foramen magnum is bordered ventrally by the basioccipital. The anterior half of the supraoccipital is overlain by the parietals. Posteriorly it abuts the epiotics and exoccipitals. Posterodorsally the bone bears a small ridge on which attaches the fascia between the two halves of the adductor mandibulae muscle A2 (see below) (Fig. 2D). The parasphenoid spans from the orbital region to the occipital region. It is a rhomboid-like bone and covers the dorsal surface of the ventroposterior tip of the premaxillo-ethmovomerine complex. It attains its maximum width near its junction with the pterosphenoid and the prootics. The parasphenoid extends caudally as two slender parasphenoidal processes from about the middle of the prootics (Figs. 2D, 3B).

The suspensorium is slightly longer than deep, resembling an inverted triangle, and consists of three robust bones (Fig. 5). The hyomandibula and quadrate are fused, forming a single, massive complex: the hyomandibulo-quadrate. The hyomandibula of the complex bears three articular condyles: the anterior suspensorial condyle articulates with the sphenotic and prootic; the posterior suspensorial condyle articulates with the pterotic; and the rostrodorsal opercular articular condyle articulates with the operculum (Figs. 3A, 5). Between the two condyles the cartilaginous dorsal edge of the hyomandibula is additionally connected by the connective tissue to the articular groove. The angular complex of the lower jaw articulates at the level of the mandibular articular facet with the quadrate by the mandibular articular condyle (Fig. 5). The palatopterygoid is reduced to a small slender bone, which lies anterior to the hyomandibulo-quadrate (Fig. 5).

The opercular bones consist of a series of four bones: operculum, preoperculum, interoperculum, and suboperculum (Figs. 3A, 5). The operculum is triangular. The dorsal process of the operculum bears the opercular articular facet for the opercular condyle of the hyomandibula. The preoperculum encloses the preoperculo-mandibular canal (Fig. 1). The dorsal process of the preoperculum is connected to the lateral side of the hyomandibula through connective tissue. Ventrocaudally, the medial side of the preoperculum is covered by and strongly attached to the interoperculum by connective tissue. The interoperculum is triangular and is strongly connected to the posterior tip of the posterior ceratohyal by connective tissue. The suboperculum is triangular and situated ventromedially to the operculum.

The anterior and largest part of the lower jaw is formed by the dento-splenio-mentomeckelian com-
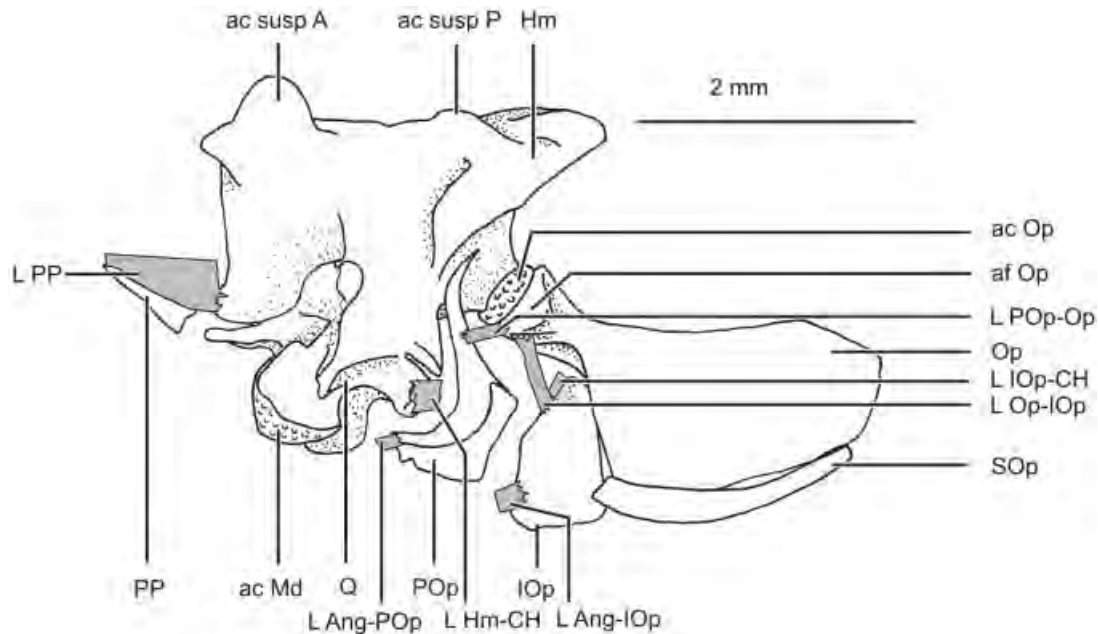
Fig. 5.   Lateral view of the suspensorium of *Moringua edwardsi*.

plex, here referred to as the dentary complex (Fig. 6A). Dorsally it bears a large coronoid process (Fig. 6A). The dentary complex is penetrated by the mandibular canal of the cranial lateral line system (Figs. 1, 2C). The coronomeckelian appears as a slender rod enclosed by the dentary complex (Fig. 2C). The posterior end of the lower jaw consists of three bones (the angular, the articular, and the retroarticular), which are fused to form the angular complex (Fig. 6A). The angular complex is pointed anteriorly and wedges into the dentary complex. Posteriorly, at three-quarters of the length of the lower jaw, the angular complex becomes exposed dorsally and medially. Caudally, the complex bears the mandibular articular facet for the quadrate (Fig. 6A). Both complexes are L-shaped in cross-section, with the horizontal ridge pointing medially.

The hyoid apparatus consists of a median basihyal; a median urohyal, with a short posterior extension; and paired anterior and posterior ceratohyals (Fig. 6B). Hypohyals and interhyals are absent.

Ligaments

The primordial ligament surrounds the caudal surface of the maxillary and extends caudally to insert on the dorsolateral face of the lower jaw (Fig. 2C). This ligament shows a extensive dorsal outgrowth, covering the anterior part of the adductor mandibulae complex and its tendons (Fig. 7). The posterior tip of the posterior ceratohyals is connected to the medial surface of the interoperculum by means of the interoperculo-ceratohyal ligament and to the hyomandibula by means of the

hyomandibulo-ceratohyal ligament (Figs. 5, 6C). A strong palatopterygoidal ligament stretches from the dorsal edge of the palatopterygoid to the parasphenoid; it more caudally connects the palatopterygoid to the anterior projection of the hyomandibulo-quadrate (Fig. 5). The dorsal edge of the interoperculum is connected through a dorsoventrally directed operculo-interopercular ligament to the ventrolateral face of the opercular dorsal process (Fig. 5). Anteriorly, a rostrocaudally directed angulo-interopercular ligament connects the anterodorsal side of the interoperculum to the ventrocaudal side of the angular complex (Figs. 5, 6A). The preoperculo-opercular ligament connects the opercular process to the caudal edge of the preoperculum (Fig. 5). The basihyo-ceratohyal ligament connects the caudolateral surface of the basihyal with the ventral surface of the anterior ceratohyals (Fig. 2C). The urohyo-ceratohyal ligament connects the anteroventral surface of the urohyal to the dorsolateral surface of the anterior ceratohyal (Fig. 2C). The angulo-preopercular ligament connects the ventrocaudal surface of the angular complex to the anterior edge of the preopercular (Figs. 5, 6A).

Myology

The adductor mandibulae complex comprises four parts: A1, A2, A3, and Aω (Fig. 7). The complex is hypertrophied so that the counterparts of A1 and A2 meet dorsally, thus covering the skull. The fibers of adductor mandibulae A1 appear as a separate, thin, and short bundle, lateral to A2. The medial fibers of A1 are connected to the tendon of the medial A2m,
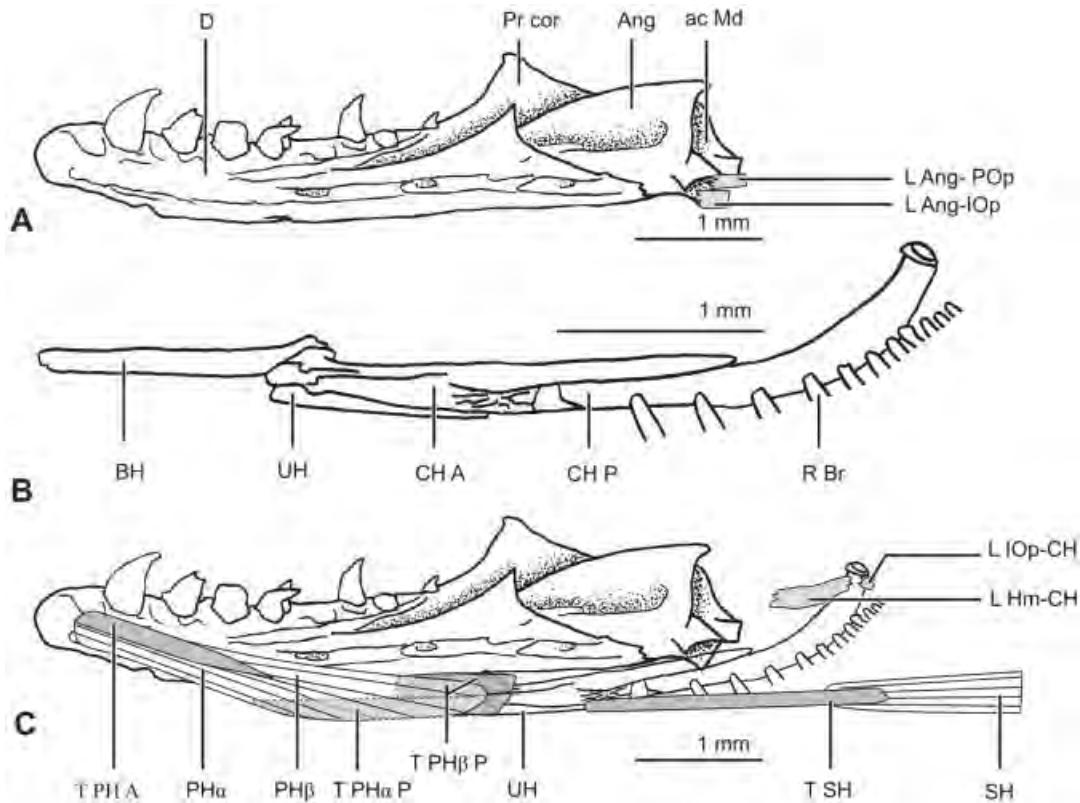
Fig. 6. **A:** Medial view of the lower jaw of *Moringua edwardsi*. **B:** Lateral view of the hyoid apparatus. **C:** Left lower jaw and left muscle bundle of the protractor hyoidei (PH) is removed. Dotted lines indicate part of the tendons being covered by the right muscle bundle.

while the ventral and lateral fibers of A1 are connected to the expanded outgrowth of the primordial ligament (Fig. 7A). The adductor mandibulae A2, comprising three bundles, is the largest part of the complex and extends dorsally and caudally. Dorsal to the neurocranium, both left and right halves of the A2 interconnect by fascia, attached to the supraoccipital (Fig. 2D). The muscular origin includes the lateral and dorsal elements of the neurocranium: frontal, pterotic, parietal, and supraoccipital. The anterodorsal part A2d is situated laterally to A3 and is covered by the tendinous plate-like extension of the primordial ligament (Fig. 7B). The fibers of A2d are ventrocaudally directed and merge into the well-developed tendon of A2m. This tendon covers the medial A2m and inserts on the posterior face of the coronoid process of the lower jaw and on the inner side of the dentary complex. The ventral part of the A2m tendon also receives fibers of the Aω, thus separating the A2m and Aω. At the level of the end of the pterotic, the caudoventral A2v is separated from A2m by an aponeurosis. The fibers of the ventral bundle A2v attach tendinously to the dorsolateral side of the hyomandibula (Fig. 2D). The adductor mandibulae A3 originates musculously from the lateroventral surface of the frontal and the pterosphenoid and extends ventrocaudally. The ventral fibers of the A3 attach to a tendon that inserts on the ventromedial ridge of the angular complex, ventromedial to the fibers of Aω. The adductor mandibulae Aω inserts on the Meckelian fossa on the medial face of the dentary and the angular complex. Fibers of Aω arise from the anteroventral part of the A2m tendon, separating Aω from A2m. More caudally, the posterior fibers of Aω and the ventral fibers of A2m interconnect. The merged fibers of A2m and Aω attach medioventrally by a tendon to the palatopterygoid, quadrate, and hyomandibula.

The levator arcus palatini runs between the suspensorium and the neurocranium (Fig. 7C). This muscle is covered laterally by the adductor mandibulae A2–Aω complex. The fibers are directed dorsoventrally and are slightly inclined caudally. The fibers merge into a tendon that originates on the lateral ridge of the sphenotic. Fibers insert on the lateral face of the hyomandibula and the quadrate.

The adductor arcus palatini runs in the roof of the buccal cavity and connects the neurocranium to the inner face of the suspensorium (Fig. 7D). The fibers are directed dorsocaudally but inclined ventrolaterally. It has muscular attachments, running from the parasphenoid to the medial side of the palatopterygoid, hyomandibula, and the quadrate. A second bundle of the adductor arcus palatini appears at the
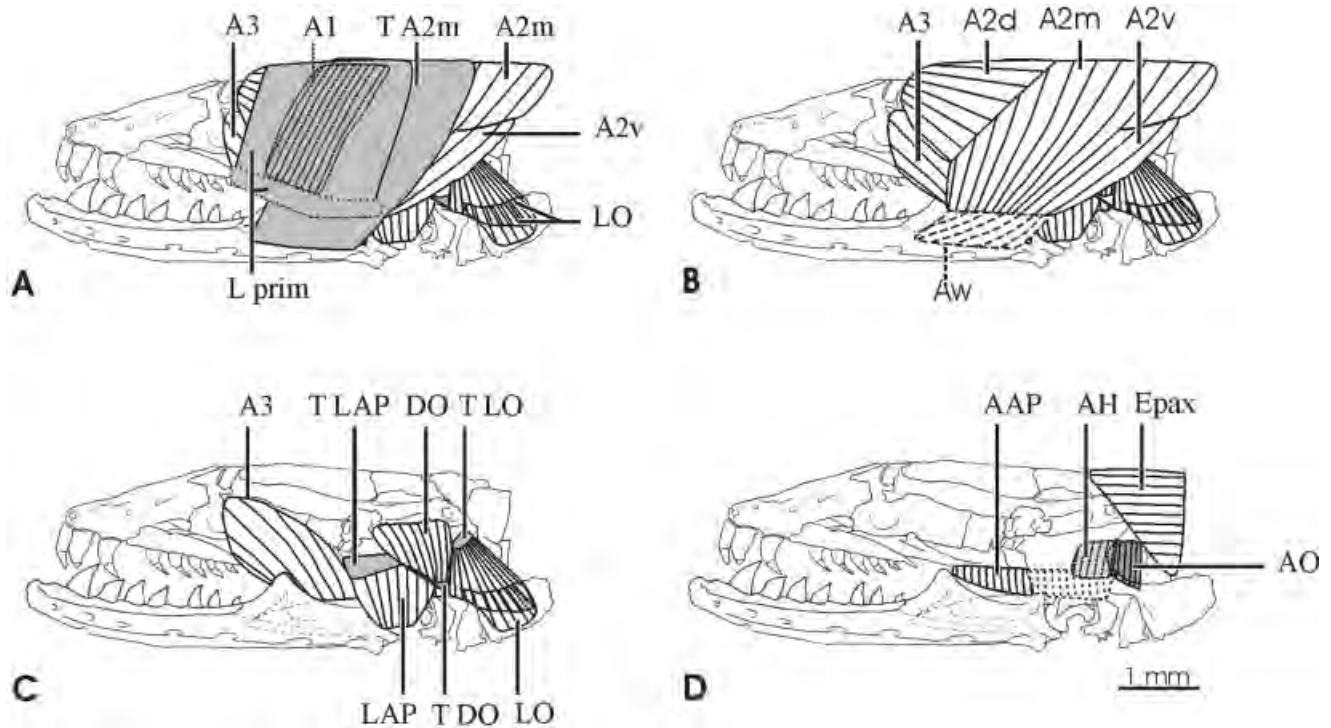
Fig. 7. Lateral view of the cranial muscles of *Moringua edwardsi*. Dotted lines indicate parts of structures being covered by other elements. **A:** Skin is removed. **B:** Primordial ligament and A1 are removed, exposing the adductor mandibulae complex with dorsal (A2d), medial (A2m), ventral (A2v), and mandibular (Aω) part. **C:** The adductor mandibulae complex is removed, except for the A3. **D:** Opercular muscles are removed.

level of the articulation between the lower jaw and the quadrate. It shows a different fiber direction and inserts on the dorsolateral face of the parasphenoid near its suture with the prootic.

The adductor hyomandibulae is situated posteriorly to the adductor arcus palatini (Fig. 7D). Its fibers attach to the dorsolateral face of the prootic and dorsolateral surface of the exoccipital (Fig. 2D). The muscular insertion sites include the dorsomedial surface of the quadrate and hyomandibula. Its anterior fibers are dorsoventrally directed, forming a right angle with the posterior fibers of the adductor arcus palatini, while a ventrolateral direction is present caudally. Posteriorly the fibers merge with the anterior fibers of the adductor operculi.

The dilatator operculi is conically shaped, with the apex lying ventrally (Fig. 7C). It is overlain laterally by the adductor mandibulae A2–Aω complex. The dorsoventrally directed fibers of the dilatator operculi attach to the posterior part of the pterotic. Its tendon borders the ventral edge of the muscle and inserts on the dorsal opercular process.

The adductor operculi covers the caudal part of the adductor hyomandibulae ventrally and can be distinguished from the latter by a different fiber direction: those of the adductor operculi are dorsoventrally directed, while the posterior fibers of the adductor hyomandibulae are directed more rostrocaudally (Fig. 2D). The fibers originate on the exoc-

cipital and insert on the dorsomedial surface of the dorsal opercular process and to the dorsomedial surface of the operculum, posterior to its articulation with the quadrate (Fig. 7D).

The levator operculi originates tendinously from the ventral face of the posterior process of the hyomandibula, near its articulation with the neurocranium (Fig. 7C). The dorsoventrally directed and caudally inclined fibers insert on the dorsal opercular process and dorsal edge of the operculum, and extend ventrally to cover its external and medial side. Some fibers even extend ventrally to insert on the lateral face of the interoperculum (Fig. 2D). The intermandibularis is absent.

The protractor hyoidei, characterized by its X-shape, connects the hyoid arch to the lower jaw. Near the dental symphysis, well-developed anterior tendons attach the right and left bundle to the medial surface of the dentary (Fig. 6C). These tendons cover the lateral surface of both bundles anteriorly. More caudally, each muscle half is divided aponeurotically into a dorsal β and ventral α part (Figs. 2C, 6C). The ventral part meets its counterpart on a median aponeurosis, forming a single unit. Both left and right parts diverge at the level of the rostral tip of the basihyal (Fig. 2C). The posterior fibers of both dorsal and ventral parts each attach to a posterior tendon. These tendons fuse to a single tendon, which

attaches to the dorsolateral surface of the anterior ceratohyal.

The sternohyoideus consists of three myomeres, separated by two myocommata. The fibers insert by means of a strong, well-developed tendon on the posterodorsal region of the urohyal (Fig. 6C). Fibers have a bipennate insertion on the tendon. The sites of origin include the medial side of the cleithrum, whereas the posterior fibers insert on a myoseptum, separating them from the hypaxial muscles.

The hyohyoideus forms a sheet of fibers that interconnects the successive branchiostegal rays (Fig. 2D). Both muscle halves continue ventrally to meet their antimeres on a ventromedial hyohyoidal myoseptum. Dorsally, fibers attach to the ventromedial side of the dorsal opercular process (Fig. 2D). Posterior to the process this muscle attaches to the medial surface of the operculum. Both muscle halves remain separate at the end of the orobranchial cavity, bordering the ventrolateral sides of each chamber. The fibers attach dorsally to the horizontal septum, between the epaxials and hypaxials, by connective tissue. Hyohyoidei abductores and inferior are absent or not differentiated. Ontogenetic series are necessary to resolve this.

The supracarinalis anterior originates from the supraoccipital and inserts on the first neural spine. The epaxials insert aponeurotically on the epiotic, the pterotic, and the supraoccipital (Figs. 2D, 7D). The myocommata between successive myomeres are visible in cross-sections. The hypaxials insert aponeurotically on the ventrocaudal border of the exoccipitals and on the basioccipal (Fig. 2D).

DISCUSSION
Morphology Related to Head-First Burrowing?

Eye reduction. Elongation of the body is rather common in fishes, amphibians, reptiles, and mammals (Lande, 1978; Hanken, 1993; Rieppel, 1996; Mecklenburg, 2003a,b) and is frequently linked to a whole set of morphological transformations. The most recurrent changes are eye reduction, increasing rigidity of the skull, increase in number of vertebrae and limblessness (Gans, 1973, 1975; Withers, 1981). Most of these changes have been linked to a burrowing lifestyle. Body elongation combined with limblessness allows unhindered movements below the substrate surface (Gans, 1975; Pough et al., 1998). Eye reduction is also believed to be related to burrowing, as well as a benthic or cryptic lifestyle (Gans, 1973, 1975; Withers, 1981; Lee, 1998). For example, eye reduction is known in anguilliform clariid catfish (*Channallabes apus*) living in submerged swamp mud (Poll, 1973; Adriaens et al., 2002); the blind spiny eel (*Caecomastacembelus brichardi*) known to inhabit rock crevices (Poll, 1973); and the blind cave salamander (*Proteus vulgaris*) (Poll, 1973). For *Moringua edwardsi,* not only does

this species show similar features, but they can also be related to an ontogenetic shift in burrowing behavior. The burrowing immature specimens have reduced eyes, whereas the pelagic adults do not (Smith, 1989a). Adults are also known to be visual predators, whereas immature specimens are believed to detect benthic and burrowing prey through olfaction and touch (Gordon, 1954; Smith, 1989a). In those immature specimens, the eyes are covered with semiopaque skin (Fig. 2Ba), which presumably has a protective role during burrowing. Protective structures for the eyes have been observed in other burrowing vertebrates as well (e.g., caecilians), but are not always related to eye reduction (e.g., some snakes and lizards; Gans, 1975).

Lateral line system. In those vertebrates in which the eyes have become completely lost, other sensory systems become more important (e.g., in fishes the lateral line system becomes the most important sensory organ for scanning the surroundings; Montgomery, 1989). In blind cave characins (*Anoptichthys jordani*), for example, the eyes are absent but the cranial lateral line system is well developed, comprising canals enclosed in bones and containing neuromasts that are in contact with the exterior through canal openings (Hassan, 1989). In *Moringua edwardsi*, however, the cranial lateral line system is markedly different: external pores are absent and canals are widened into dermal cavities. Even though the connection with the exterior seems to be lost, the neuromasts are still well developed. We hypothesize that the lack of pores is a specialization for burrowing, as this avoids the entering of sediment into the canals during head-first burrowing. The dermal cavities may function as a kind of sensory pads that are stimulated mechanically during burrowing or when in contact with prey, subsequently pushing fluid into the canals and thus stimulating the neuromasts in the canals (J. Webb, pers. commun.).

Jaw adductor hypertrophy. The reduction of the eye, especially in a macropthalmic ancestral state, can be expected to have a substantial impact on the spatial design of the head. In anguilliform clariids, hypertrophy of the jaw muscles has been linked to reduction of the eyes (Devaere et al., 2001). We may assume that in *Moringua edwardsi* the reduced eyes similarly create space allowing the expansion of the adductor mandibular muscles (+ unusual orientation of fibers; see below). Hypertrophy of jaw adductor muscles has been linked before to either head-first burrowing (Atkinson and Tayler, 1991; Nelson, 1994) or a predatory life style (Helfman et al., 1997; Parmentier et al., 1998).

Hypertrophied mouth-closing muscles suggest the ability for powerful biting, with a consequent increase of mechanical loads on skeletal elements (Herrel et al., 2002; Van Wassenbergh et al., 2004). The link with predation has been made for muraenids, which also show structural adaptations in

the dental coronoid process and suspensorium (Böhlke et al., 1989). It is possible that the presence of hypertrophied jaw muscles is the plesiomorphic state in the order Anguilliformes, since a predatory lifestyle represents the primitive condition of the Anguilliformes (Gosline, 1971; Smith, 1989b), since hypertrophied jaw muscles and a strong bite are advantageous for predation, and since hypertrophied jaw muscles are frequent in Anguilliformes (e.g., in Anguillidae, Muraenidae, Congridae, Ophichthidae, etc.). Of course, such assumptions have to be taken carefully and a cladistic analysis has to be performed to test this. *Monopterus* and *Synbranchus*, which are also eel-shaped burrowers, show striking convergence in the hypertrophy and fiber direction of the adductor mandibulae complex, shape, and size (reduced) of the opercular apparatus and shape and orientation of the levator operculi. These features have been linked before to their specialized predacious feeding mode (Liem, 1980). In *Moringua edwardsi*, the hypertrophied jaw muscles are likely to be advantageous in head-first burrowing as well.

Head-first burrowing can occur through mouth excavation (e.g., *Cepola rubescens*) or through shoveling movements of the snout, in which both forward forces are generated through body undulations (Castle, 1968; Smith, 1989a,b; Atkinson and Tayler, 1991). *Moringua edwardsi* is known to penetrate the substrate with its conical snout and protruding lower jaw, without actual oral excavation. Consequently, powerful biting during excavation cannot explain the presence of the hypertrophied jaw muscles in *M. edwardsi*, even though a very large coronoid process and rigid suspensorium (to which the jaw muscles attach) are present. Still, as these muscles substantially enclose the posterior part of the skull, they may reinforce the lower jaw during shoveling, thereby protecting it from disarticulation (see below). Also, as a gap between the jaw adductors and epaxials is absent, because of them interconnecting, the transition from head to body is smooth (thus improving substrate penetration).

Several additional features in *Moringua edwardsi* can be linked to a predatory life style, apart from jaw muscle hypertrophy. Some examples are the large recurved teeth on the upper and lower jaws (including vomeralis), robust upper and lower jaws for holding prey, and a large gape. The robustness of the upper jaw results from the fusion of the premaxillary, ethmoid, and vomer to form the premaxilloethmovomerine complex. Even though this fusion is synapomorphic for Anguilliformes, it is assumed to be a specialization for predatory feeding (Eaton, 1935; Gosline, 1980; Smith, 1989a). In those teleosts, handling of prey occurs through rotational feeding, inducing large torque forces onto the skull. Structural changes for resisting these forces can thus be expected, both at the skeletal and myological level (see below).

Hyperossification. Apart from structural reinforcements to deal with increasing loads during jaw adductor contraction, elevated levels of ossification have been associated directly to head-first burrowing as well (Rieppel, 1996; Lee, 1998). Amphisbaenids, uropeltid, and scolecophid snakes, caecilia (Gans, 1975; Hanken, 1983; Duellman and Trueb, 1986), and even some frogs (e.g., *Hemisus*; Pough et al., 1998), which are true head-first burrowers, show extreme skull modifications that can be linked to resisting compressive forces during burrowing. Not only the bones themselves but also connections between bones contribute to skull strength. The distribution of different types of joints (e.g., scarf or butt joints) or fusions between bones may reflect the presence of high mechanical loadings (Duellman and Trueb, 1986; Hildebrand, 1995) (Fig. 4). In *Moringua edwardsi*, fusions occur in the upper jaw (forming the solid premaxillo-ethmovomerine complex), and scarf joints, with large overlaps between bones, are present between most bones in the skull roof (Fig. 2Bb,c). The large interorbital distance, as a result of the reduced eyes and consequently reduced orbits, also improves skull fortification.

Morphology Related to Miniaturization?

Morphological transformations related to miniaturization, rather than to head-first burrowing, cannot be excluded, as miniaturization frequently occurs in burrowing vertebrates (Hanken, 1993; Rieppel, 1996). Elongation of the body, reduction of limbs, and dental and cranial transformation (reduction in skull size, hypertrophy of the adductor mandibulae complex, hyperossification) are also characteristic features of many miniaturized taxa, including caecilia (e.g., *Idiocranium russelli*) and lizards (e.g., *Dibamus novaeguineae*; Hanken, 1993). Hyperossification is frequently interpreted as compensation for mechanical weakening (due to decrease in body size and reduction of bones). Large coronoid processes have also been explained in the context of miniaturization. Isometric reduction of skull size would imply shortening of jaw muscle fibers, thus compromising their functionality (Hanken, 1993). The formation of a higher coronoid process, combined with a posterior expansion of jaw muscle insertion, increases biting force within a smaller spatial design. Rieppel (1996) concludes, however, that such cranial transformations in miniaturized lizards are consequences of a burrowing lifestyle and not due to miniaturization. However, for *Moringua edwardsi* it is not clear whether the observed features are related to one of both, or both. The fact that pedomorphosis, which frequently co-occurs with miniaturization (Rieppel, 1996), seems to be absent in *M. edwardsi*, might suggest a closer relation with the burrowing (and feeding) lifestyle.
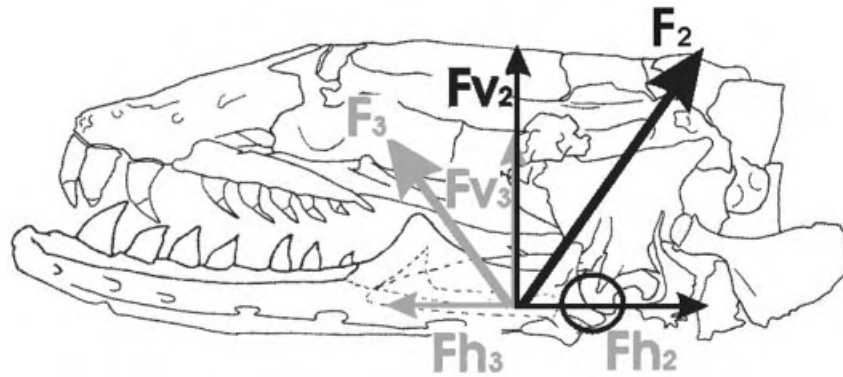
Fig. 8. Schematic illustration of the generated forces by the adductor mandibulae A2 (F2) and A2 (F3) with, respectively, their horizontal (Fh 2 and Fh 3) and vertical components (Fv 2 and Fv 3). The horizontal components run in the opposite direction, reducing the pressure in the joint between the lower jaw and the quadrate (encircled).

Morphology Related to Feeding Habits and Prey Capture?

Rotational feeding. As mentioned above, limb-lessness and body elongation in vertebrates frequently co-occurs with rotational feeding and has been observed both in teleosts (e.g., *Anguilla anguilla*) and tetrapods (e.g., caecilians) (Duellman and Trueb, 1986; Helfman and Clark, 1986). Here, spinning movements of the elongated body are coupled to a powerful grasping of the prey. The physical coupling of epaxials and jaw muscles could thus be considered an advantage for transferring forces from the body onto the head. The insertion of the lateral fibers of the epaxials onto an aponeurosis, separating it from the jaw muscles, has been observed in caecilians, *Anguilla anguilla* and *Monopterus* (Liem, 1980). The same is the case for *Moringua edwardsi*. Additionally, in this species the spatial constraints for the insertion of the epaxials, due to the jaw muscle hypertrophy, are circumvented by the expansion of the latter aponeurosis (Fig. 2D).

Rotational feeding also requires a solid grip onto the prey, which is enhanced in caecilians, *Anguilla anguilla*, and in *Moringua edwardsi* due to the presence of recurved teeth on both upper and lower jaws. However, a solid grip during rotations requires an increased structural rigidity of the jaws to resist torque forces, especially at the level of their attachment onto the neurocranium. The fusion of the upper jaw bones (see above), as well as the neurocranium, solid lower jaw, and suspensorium can assist in resisting these forces. The absence of a direct, rigid connection between the anterior part of the suspensorium and the neurocranium (as the palatopterygoid has become decoupled from the hyomandibulo-quadrate) may seem to contradict this. However, modeling of forces has shown that in catfishes, which also lack this connection, the suspensorium and lower jaw articulation can resist elevated forces simply by the way they are positioned and shaped (Herrel et al., 2002). The occurrence of the extensive lap joints in the skull roof of *M. ed-*

wardsi undoubtedly attribute to the neurocranial rigidity.

The lower jaw may also be prevented from being dislodged thanks to the hypertrophied jaw muscle complex, in combination with the large coronoid process. Not only the jaw muscle size, but also the orientation of the different bundles composing this complex may contribute (Fig. 7B). A surprising feature of the jaw muscle morphology is the anteriorly directed A2d and A3, combined with the posteriorly directed A2m and A2v (Fig. 7B). Consequently, their corresponding forces, i.e., F3 and F2, respectively, generate an adduction component (F2v and F3v) and a component working onto the lower jaw articulation (F2h and F3h) (Fig. 8). The latter two thus point in opposite directions and partially neutralize each other. This prevents dislocation of the joint, even though large forces are exerted that can assist in resisting torque forces during rotational feeding (P. Aerts, pers. commun.). Rotational feeding is known for *Monopterus* and *Synbranchus* as well (Liem, 1980). The morphological convergence with *Moringua edwardsi* is striking: the adductor mandibulae complex is hypertrophied and the anterior fibers of the A2 are anteriorly directed as well. The statement of Liem (1980, p. 322) considering rotational feeding in *Monopterus* "Once prey is captured, the highly hypertrophied adductor mandibulae complex plays a key role in conjunction with the corkscrew-like twisting motion of the body in breaking up the prey into pieces" confirms our assumptions.

Body elongation, reduction of the eyes, modified cranial lateral line system, and modified skull shape (pointed though firm) can be considered specializations with respect to head-first burrowing. Hyperossification can probably be regarded more of a specialization for head-first burrowing and feeding, even though an impact of miniaturization cannot be excluded. Hypertrophied adductor mandibulae muscles and the enlarged coronoid process can be associated with both feeding requirements (enables bite forces necessary for their predatory behavior) and

with a burrowing lifestyle, as well as miniaturization.

ACKNOWLEDGMENTS

LITERATURE CITED

Adriaens D, Devaere S, Teugels GG, De Kegel B, Verraes W. 2002. Intraspecific variation in limblessness in vertebrates: a unique example of microevolution. Biol J Linn Soc 75:367–377.

Atkinson RJA, Tayler AC. 1991. Burrows and burrowing behaviour of fish. Symp Zool Soc Lond 63:133–155.

Böhlke EB, McCosker JE, Böhlke JE. 1989. Family Muraenidae. In: Böhlke EB, editor. Fishes of the western North Atlantic. New Haven, CT: Sears Foundation for Marine Research. p 104–206.

Castle PHJ. 1968. A contribution to a revision of the moringuid eels. Special Publication 3. Grahamstown, South Africa: Rhodes University Department of Ichthyology. p 1–29.

Devaere S, Adriaens D, Verraes W, Teugels GG. 2001. Cranial morphology of the anguilliform clariid *Channallabes apus* (Günther, 1873) (Teleostei: Siluriformes): adaptations related to a powerful biting? J Zool (Lond) 255:235–250.

Duellman WE, Trueb L. 1986. Musculoskeletal system. In: Duellman WE, Trueb L, editors. Biology of amphibians. New York: McGraw-Hill. p 289–364.

Eaton TH Jr. 1935. Evolution of the upper jaw mechanism in teleost fishes. J Morphol 58:157–172.

Gans C. 1973. Locomotion and burrowing in limbless vertebrates. Nature 242:414–415.

Gans C. 1975. Tetrapod limblessness: evolution and functional corollaries. Am Zool 15:455–467.

Gordon SM. 1954. The eel genus Stilbiscus. Copeia 1:11–15.

Gosline WA. 1956. The Hawaiian fishes of the family Moringuidae: another eel problem. Copeia 1:9–18.

Gosline WA. 1965. Teleostean phylogeny. Copeia 1:186–194.

Gosline WA. 1980. The evolution of some structural systems with reference to the interrelationships of modern lower teleostean fish groups. Jpn J Ichthyol 21:1–24.

Gregory WK. 1933. Fish skulls: a study of the evolution of natural mechanisms. Trans Am Philos Soc 23:75–481.

Hanken J. 1983. Miniaturization and its effects on cranial morphology in plethodontid salamanders, genus *Thorius* (Amphibia, Plethodontidae). II. The fate of the brain and sense organs and their role in skull morphogenesis and evolution. J Morphol 177:255–268.

Hanken J. 1993. Adaptation of bone growth to miniaturization of body size. In: Hall BK, editor. Bone: bone growth, vol. 7. Boca Raton, FL: CRC Press. p 79–104.

Hanken J, Wassersug R. 1981. The visible skeleton. A new double-stain technique reveals the nature of the "hard" tissues. Funct Photogr 16:22–26.

Hassan ES. 1989. Hydrodynamic imaging of the surroundings by the lateral line of the blind cave fish *Anoptichthys jordani*. In: Coombs S, Görner P, Münz H, editors. The mechanosensory lateral line. New York: Springer.

Helfman GS, Clark JB. 1986. Rotational feeding: overcoming gape-limited foraging in anguillid eels. Copeia 3:679–685.

Helfman GS, Collette BB, Facey DE. 1997. Functional morphology of locomotion and feeding. In: Helfman GS, Collette BB, Facey DE, editors. The diversity of fishes. London: Blackwell Science. p 101–116.

Herrel A, Adriaens D, Verraes W, Aerts P. 2002. Bite performance in clariid fishes with hypertrophied jaw adductors as deduced by bite modelling. J Morphol 253:196–205.

Hildebrand CM. 1995. Analysis of vertebrate structure, 4th ed. New York: John Wiley & Sons.

Lande R. 1978. Evolutionary mechanisms of limb loss in tetrapods. Evolution 32:73–92.

Lee MSY. 1998. Convergent evolution and character correlation in burrowing reptiles: towards a resolution of squamate relationships. Biol J Linn Soc 65:369–453.

Liem KF. 1980. Acquisition of energy by teleosts: adaptive mechanisms and evolutionary patterns. In: Ali MA, editor. Environmental physiology of fishes. New York: Plenum. p 299–334.

Lundberg JG, Baskin JN. 1969. The caudal skeleton of the catfishes, order Siluriformes. Am Mus Novitat 2398:1–19.

Mecklenburg CW. 2003a. Family Ptilichthyidae Jordan and Gilbert 1883 — Quillfishes. Calif Acad Sci Annot Checklists Fishes 12:1–3.

Mecklenburg CW. 2003b. Family Scytalinidae Jordan and Evermann 1898 — Graveldivers. Calif Acad Sci Annot Checklists Fishes 11:1–3.

Monod T. 1968. Le complexe urophore des poissons téléostéens. Mémoires de l' Institut Fondamental d'Afrique Noire 81:1–705.

Montgomery JC. 1989. Lateral line detection of planktonic prey. In: Coombs S, Görner P, Münz H, editors. The mechanosensory lateral line. New York: Springer.

Nelson JN. 1994. Fishes of the world. New York: John Wiley & Sons.

Parmentier E, Chardon M, Poulicek M, Bussers JC, Vandewalle P. 1998. Morphological particularities of the head in four Carapidae (Ophidiiformes). Abstract book, European Meeting of the International Society for Reef Studies. p 135–146.

Poll M. 1973. Les yeux des poissons aveugles Africains et de *Caecomastacembelus brichardi* Poll en particulier. Annales du Spéléologie 28:221–230.

Pough HF, Andrews RM, Cadle JE, Crump ML, Savitzky AH, Wells KD. 1998. Body support and locomotion. In: Pough HF, editor. Herpetology. Englewood Cliffs, NJ: Prentice Hall.

Regan CT. 1912. The osteology and classification of the teleostean fishes of the order Apodes. Ann Mag Nat Hist 8:377–387.

Rieppel OC. 1996. Miniaturization in tetrapods: consequences for skull morphology. In: Miller PJ, editor. Miniature vertebrates. Oxford: Clarendon Press. p 15–45.

Smith DG. 1989a. Family Moringuidae. In: Böhlke EB, editor. Fishes of the western North Atlantic. New Haven, CT: Sears Foundation for Marine Research. p 55–71.

Smith DG. 1989b. Family Heterenchelyidae. In: Böhlke EB, editor. Fishes of the western North Atlantic. New Haven, CT: Sears Foundation for Marine Research. p 48–54.

Smith DG, Castle PHJ. 1972. The eel genus *Neoconger* Girard: systematics, osteology, and life history. Bull Mar Sci 22:196–249.

Trewavas E. 1932. A contribution to the classification of the fishes of the order Apodes, based on the osteology of some rare eels. Proc Zool Soc (Lond) 43:639–659.

Van Wassenbergh S, Herrel A, Adriaens D, Aerts P. 2004. Effects of jaw adductor hypertrophy on buccal expansions during feeding of airbreathing catfishes (Teleostei, Clariidae). Zoomorphology 123:81–93.

Winterbottom R. 1974. A descriptive synonymy of the striated muscles of the Teleostei. Proc Acad Nat Sci Phil 125:225–317.

Withers PC. 1981. Physiological correlates of limblessness in fossorial lizards. Copeia 1:197–204.